ACS Macro Letters

Letter

pubs.acs.org/macroletters

Hexanoyl-Chitosan-PEG Copolymer Coated Iron Oxide Nanoparticles for Hydrophobic Drug Delivery

Meng-Hsuan Hsiao,[†,‡,§] Qingxin Mu,[†,§] Zachary R. Stephen,[†] Chen Fang,[†,∥] and Miqin Zhang*[,†]

[†]Department of Materials Science and Engineering, University of Washington, Seattle, Washington 98195, United States
[‡]Department of Materials Science and Engineering, National Chiao Tung University, Hsinchu City 300, Taiwan
[∥]Clinical Research Division, Fred Hutchinson Cancer Research Center, Seattle, Washington 98109, United States

Supporting Information

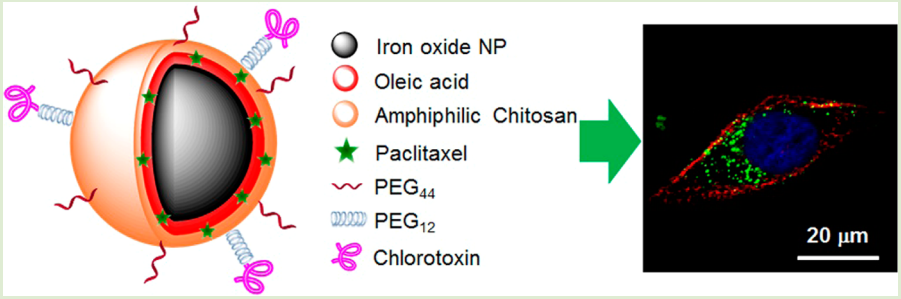

ABSTRACT: Nanoparticle (NP) formulations may be used to improve in vivo efficacy of hydrophobic drugs by circumventing solubility issues and providing targeted delivery. In this study, we developed a hexanoyl-chitosan-PEG (CP6C) copolymer coated, paclitaxel (PTX)-loaded, and chlorotoxin (CTX) conjugated iron oxide NP (CTX-PTX-NP) for targeted delivery of PTX to human glioblastoma (GBM) cells. We modified chitosan with polyethylene glycol (PEG) and hexanoyl groups to obtain the amphiphilic CP6C. The resultant copolymer was then coated onto oleic acid-stabilized iron oxide NPs (OA-IONP) via hydrophobic interactions. PTX, a model hydrophobic drug, was loaded into the hydrophobic region of IONPs. CTX-PTX-NP showed high drug loading efficiency (>30%), slow drug release in PBS and the CTX-conjugated NP was shown to successfully target GBM cells. Importantly, the NPs showed great therapeutic efficacy when evaluated in GBM cell line U-118 MG. Our results indicate that this nanoparticle platform could be used for loading and targeted delivery of hydrophobic drugs.

Many potent therapeutic compounds, such as paclitaxel (PTX), encounter delivery issues due to poor water solubility. To improve solubility of these hydrophobic molecules, various formulations of nanoparticles have been developed in the past decades, many of which were liposome and micelle-based.[1,2] However, the large size of liposomes (usually >100 nm), the low drug loading efficiency of micelles, and the stability concern for the both formulations limit their application.[3−5] Novel multifunctional nanoparticles (NPs) combining diagnostic imaging and therapeutic delivery have emerged as a powerful solution for future cancer therapy in recent years.[6,7] Among many types of NPs investigated, iron oxide NPs (IONPs) are an attractive candidate due to their biocompatibility and biodegradability. Moreover, IONPs have intrinsic superparamagnetic properties that provide excellent contrast in magnetic resonance imaging (MRI) and have shown the ability to cross biological barriers. Because of these unique features, IONPs have become an important platform for development of nanoparticle-based formulations for cancer diagnosis and therapy.[8]

An appropriate surface coating is imperative to preventing aggregation of NPs and providing additional functionality such as tissue specific targeting and improved drug loading efficiency. Various types of materials have been investigated for hydrophilic IONP coating, such as polyethylene glycol (PEG),[9] dextran,[10] phospholipids,[11] and recently, chitosan.[12,13] Chitosan is a biocompatible and biodegradable linear polysaccharide, composed of β-1,4-linked 2-amino-2-deoxy-D-glucopyranose units. It is recognized as a biomaterial for medical applications.[14−17] Furthermore, chitosan can be chemically modified with various functional molecules such as targeting ligands and therapeutic agents through its abundant primary amine groups.[18,19]

To overcome the challenges in hydrophobic drug delivery and provide imaging capabilities, we utilized the advantages of IONPs and chitosan to fabricate a PTX-loaded, amphiphilic triblock hexanoyl-chitosan-PEG (CP6C) copolymer coated, and chlorotoxin (CTX)-conjugated NP (CTX-PTX-NP). CTX is a 36-amino acid peptide and specifically binds to matrix metalloproteinase-2 (MMP-2) that is overexpressed on majority of primary brain tumors but not healthy brain

Received: February 5, 2015
Accepted: March 17, 2015
Published: March 23, 2015

DOI: 10.1021/acsmacrolett.5b00091
ACS Macro Lett. 2015, 4, 403−407

tissues.[20,21] CTX was used for targeting of human glioblastoma (GBM) cells in this study.

Methoxy PEG (mPEG)-modified chitosan (CP) was first synthesized following a previously reported procedure.[22,23] CP was further modified with a six-carbon chain using hexanoic anhydride (Figure 1a). Hydrophobic interactions of the carbon

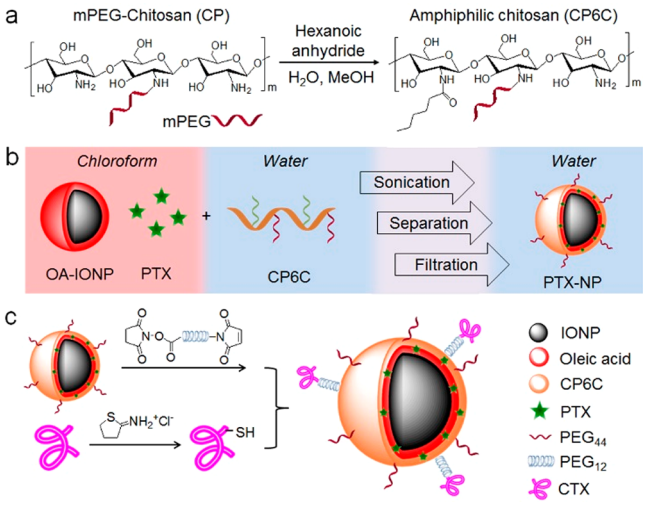

Figure 1. Preparation of CP6C copolymer-coated, PTX loaded, and CTX conjugated IONPs. (a) Synthesis of copolymer. (b) Preparation of PTX-NP. (c) Conjugation of CTX onto PTX-NP.

chains on the copolymer with the carbon chains of oleic acid on oleic acid-stabilized IONPs (OA-IONP) facilitated the phase transfer of PTX-NP from chloroform to water. The chloroform was then evaporated after ultrasonication. The NP solution was separated and filtered through a 0.2 μm polytetrafluoroethylene syringe filter to remove aggregates (Figure 1b). CTX was conjugated onto PTX-NP to obtain CTX-PTX-NP (Figure 1c) and the product was purified using PD-10 column equilibrated with PBS (Supporting Information, section 1.5).

The molecular structures of the polymers were characterized using FT-IR and NMR. The FT-IR spectra are shown in Figure 2a. After conjugation of mPEG, there were three additional peaks at 1241, 1280, and 1344 cm^{-1} from the CP sample corresponding to C−O stretching from mPEG, confirming that mPEG was successfully conjugated onto chitosan. FTIR characterization of CP modified with a six-carbon chain through reaction with hexanoic anhydride showed two peaks at 1651 and 1740 cm^{-1} corresponding to amide and ester groups, respectively. The two peaks indicate hexanoic anhydride conjugated with the amine groups and hydroxide groups on CP to form amide and ester linkages.

The triblock copolymer CP6C was also characterized by ^{1}H NMR (Figure 2b). The characteristic peaks of CP6C including the methyl ($-CH_3$) and methylene ($-CH_2-$) of the hexanoyl group clearly appear in the NMR spectra at 0.765 (ε), 1.192 (γ), 1.234 (δ), 1.489 (β), and 2.187 (α) ppm. In the spectrum, the peaks from mPEG were present at 2.619 (PEG-CH_2-CO-NH-, triplet) and 1.208 (methyl proton from mPEG) ppm. The peaks around 4−5 ppm may refer to H1 hydrogens on acetylated rings and deacetylated rings[24−26] with modifications of hexanoyl and mPEG groups. These results confirm that the mPEG and six-carbon chain were chemically bonded along the chitosan backbone. The degree of substitution (DS) of the six-carbon chain was estimated using following equation:

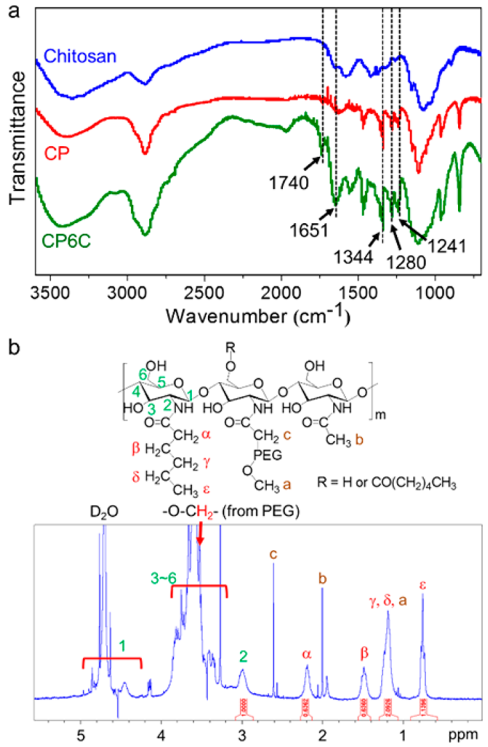

Figure 2. Characterization of polymers. (a) FT-IR spectra of chitosan, CP and CP6C. (b) ^{1}H NMR characterization of CP6C.

$$\text{DS\%} = \frac{\text{integrated area of}(\alpha+\beta)/\text{No. of hydrogens at}(\alpha+\beta)}{\text{integrated area of } \mathbf{2}/\text{No. of hydrogens at } \mathbf{2}} \times 100\%$$

The DS of six-carbon chain on CP6C was calculated to be 31.8%. The short chain chitosan had ~25 glucopyranose units per chain, yielding ~8 hydrophobic branches on each chitosan chain. The DS of mPEG was calculated to be ~14.4% (~3.6 mPEG per chitosan chain) according to the ^{1}H NMR spectrum of CP (Supporting Information, Figure S1) by using trimethylsilyl propanoic acid as an internal reference. After CP6C was synthesized and characterized, we coated the copolymer on IONPs and loaded PTX concurrently through hydrophobic interactions between PTX, the six-carbon chain of the copolymer, and oleic acid of IONPs.

A TEM image of PTX-NP with negative staining is shown in Figure 3a. Bright circles around IONPs were clearly observed, which was due to unstained copolymers coated on IONPs surface. The evaluation of the core size of PTX-NP from TEM images showed the majority of NPs to be ~11 nm in diameter (Figure 3b). The coating enhanced solubility and stability of IONP in water and buffer solutions due to good water solubility of the copolymer. To optimize loading of the copolymer and PTX onto NPs, we selected three different CP6C/IONP ratios and determined their size, encapsulation efficiency (EE%), and ξ-potential. The hydrodynamic sizes of the NPs coated with less copolymer (CP6C/IONP = 0.5:1 and 1:1, mass ratio) were smaller (28.2 and 30.8 nm) initially, but gradually increased to 52.3 and 59.8 nm, respectively, after incubation. On the other hand, the NP coated with more copolymer (CP6C/IONP = 2:1) had an initial diameter of 50.8 nm and increased slightly to 53.1 nm after a four-week incubation at 37 °C (Figure 3c,e).

Due to hydrophobic interactions, the six-carbon chain of CP6C and oleic acid of OA-IONP form a lipophilic interface that can stabilize hydrophobic chemicals in water. Therefore,

DOI: 10.1021/acsmacrolett.5b00091
ACS Macro Lett. 2015, 4, 403−407

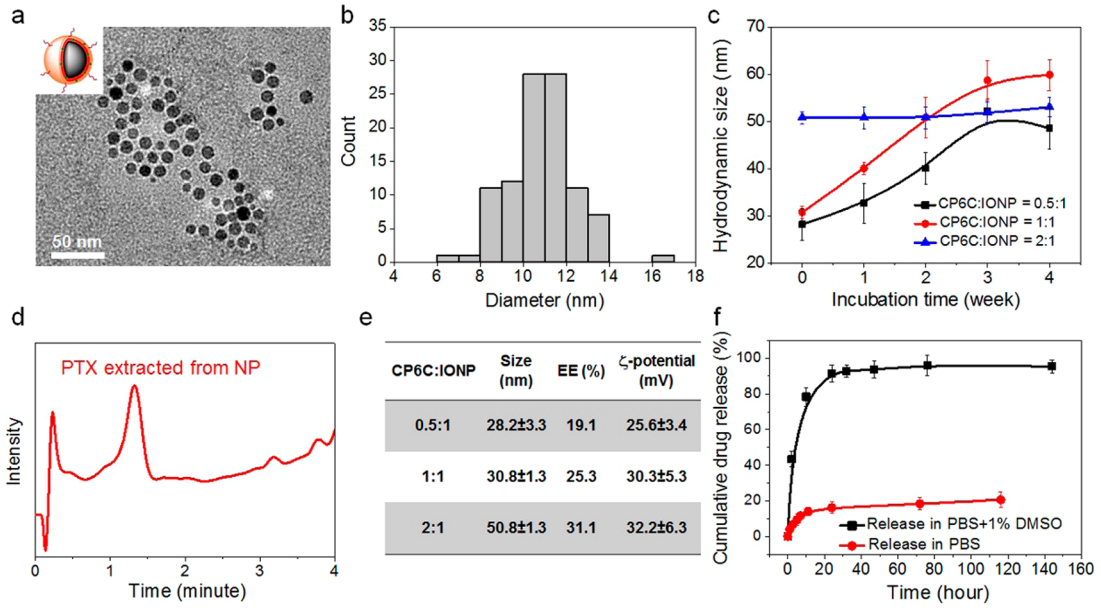

CP6C:IONP	Size (nm)	EE (%)	ζ-potential (mV)
0.5:1	28.2±3.3	19.1	25.6±3.4
1:1	30.8±1.3	25.3	30.3±5.3
2:1	50.8±1.3	31.1	32.2±6.3

Figure 3. Characterization of NPs. (a) TEM micrograph of PTX-NP. (b) Histogram of NP core size distribution. (c) Effect of CP6C/IONP ratio on stability of NPs. (d) Quantification of PTX on PTX-NP by HPLC. (e) Effect of CP6C/IONP ratio on properties of NPs. (f) Cumulative drug release of PTX from PTX-NP in PBS and PBS + 1% DMSO.

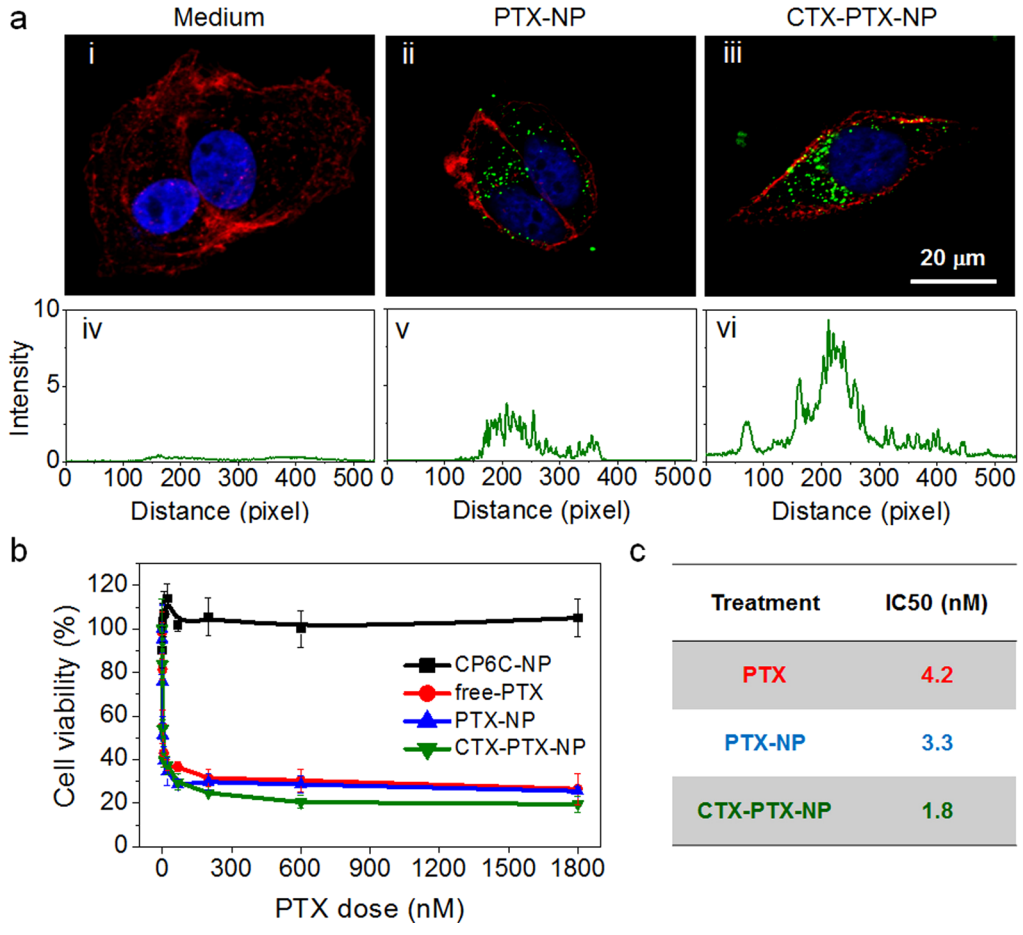

Treatment	IC50 (nM)
PTX	4.2
PTX-NP	3.3
CTX-PTX-NP	1.8

Figure 4. Evaluation of cellular uptake and drug efficacy of NPs. (a) Cellular uptake of PTX-NP and CTX-PTX-NP ([Fe] = 40 μg/mL) after 6 h incubation, examined by CLSM. (i–iii) Confocal micrographs; (iv–vi) Profiles of green fluorescence intensity quantified by ImageJ. (b) Viability of U-118 MG cells after 72 h treatment with free PTX, CP6C-NP, PTX-NP, and CTX-PTX-NP, respectively. (c) IC_{50} values of free PTX, PTX-NP, and CTX-PTX-NP.

DOI: 10.1021/acsmacrolett.5b00091
ACS Macro Lett. 2015, 4, 403–407

this platform could be employed as a drug carrier for various hydrophobic drugs. In this study, PTX was added in the OA-IONP/chloroform solution before addition of the CP6C solution. The drug was then encapsulated into the hydrophobic interface between the copolymer and IONP during the microemulsion process and purified by size exclusion chromatography in to PBS.

To examine loading of PTX, chloroform was used to extract PTX from PTX-NP. HPLC was used to identify and quantify PTX in the extract (Figure 3d). The chromatograph indicated that PTX was successfully loaded onto NPs. The PTX encapsulation efficiency for PTX-NP after purification was 31.1 ± 2.2 μg/mL, and the concentration of iron oxide of PTX-NP was 78 ± 4.3 μg/mL, as determined by the ferrozine assay, yielding a drug encapsulation efficiency of 31.1% for PTX-NP with a CP6C/IONP ratio of 2:1. The drug encapsulation efficiency of PTX-NP with lower ratios of CP6C/IONP were also measured, which yielded a loading efficiency of 19.1% for PTX-NP with a CP6C/IONP ratio of 0.5:1 and 25.3% for PTX-NP with a ratio of 1:1 (Figure 3e). Since synthesis of PTX-NP with a 2:1 CP6C/IONP ratio increased the transfer efficiency of IONPs from the organic phase to the water phase, enhanced drug loading, and increased stability, PTX-NP with a ratio of CP6C/IONP 2:1 was used in the following studies. The encapsulation efficiency results indicate that increasing the copolymer to IONP ratio clearly increased PTX loading (Figure 3e). ξ-Potential also increased indicating more positively charged chitosan was coated onto the NPs. The above discussion suggests that increasing the amount of CP6C coating enhanced drug loading and stability of PTX-NP in PBS at 37 °C and PTX-NP with CP6C/IONP ratio of 2:1 provides the most desirable NP properties for our intended application and thus is used in the following studies.

The drug release profile of PTX-NP was measured in PBS and PBS plus 1% DMSO (Figure 3f). The PTX release rate from PTX-NP in pure PBS was very low, with 16% of PTX released from the PTX-NP after 1 day and less than 20% after 5 days, indicating that the NP prevented rapid release of PTX in an aqueous environment. PTX-NP in PBS plus 1% DMSO showed a rapid release of PTX in the first 24 h, with over 91% of PTX released. This result suggests that, at physiological pH, PTX would release in an environment with reduced polarity, such as cell membrane lipid bilayers.[27,28] However, the release mechanisms in biological systems such as cells are poorly understood and need to be further investigated.

The stability of PTX-NP in serum was also examined. NPs were incubated in 50% fetal bovine serum in PBS at 37 °C for 1 week. No apparent change in hydrodynamic size of NPs was observed, indicating that NPs had excellent stability (Supporting Information, Figure S2). In contrast, most liposomes remain stable in serum at 37 °C for only a few hours.[29−31]

PTX-NP was conjugated with CTX (CTX-PTX-NP) to target U-118 MG cells (Supporting Information, section 1.5). To evaluate the biological effect of CTX-PTX-NP, we used a human GBM cell line U-118 MG as target cancer cells. We first studied cellular uptake of NPs by confocal laser scanning microscopy (CLSM). PTX-NP and CTX-PTX-NP were modified with NHS-fluorescein to visualize NP uptake with fluorescence imaging. PTX-NP and CTX-PTX-NP with same iron content (40 μg/mL) were added to U-118 MG cells and incubated for 6 h. Figure 4a shows cell images after incubation with NPs. Although nonspecific uptake of PTX-NP by cells was observed, much more CTX-PTX-NP was taken up by cells, indicating that the conjugation of CTX improved cellular uptake. The green fluorescence intensities on the images were quantified and results showed that the fluorescence intensity from CTX-PTX-NP was significantly higher than that from PTX-NP (Figure 4a, v and vi). This result implicates that CTX-PTX-NP might have better therapeutic efficiency in killing U-118 MG cells than free-PTX and PTX-NP.

Next, viability of U-118 MG cells was tested by the Alamar Blue assay. Cells were treated for 72 h with CP6C-NP, free PTX, PTX-NP, and CTX-PTX-NP to determine biocompatibility of CP6C-NP control and to compare the therapeutic efficacy of PTX NP formulations against free PTX over a range of concentrations (Figure 4b). The CP6C-NP (treatments at same Fe concentration as PTX NP formulations) exhibited low cytotoxicity without PTX loading, showing the biocompatibility of the base NP formulation (i.e., NPs with no drug and targeting ligand). Using the cell viability curves, the IC_{50} values for free-PTX, PTX-NP, and CTX-PTX-NP were calculated to be 4.2, 3.3, and 1.8 nM, respectively. CTX-PTX-NP had better therapeutic efficiency in U-118 MG cells at high PTX concentrations than free-PTX and PTX-NP. CTX is known to bind with MMP-2 on GBM cells.[21] Our previous studies have shown that CTX-conjugated NPs were able to target GBM cells in vitro and in vivo.[20] Therefore, the enhanced tumor cell killing was likely due to improved cellular drug accumulation mediated by CTX in CTX-PTX-NP.

In summary, CP6C was synthesized successfully and the molecular structure was characterized by FT-IR and NMR. The copolymer was successfully used to coat OA-IONP by hydrophobic interaction between six-carbon chains on the copolymer and the oleic acid layer on the IONP, and hydrophobic interface was used to encapsulate PTX for drug delivery. The obtained base nanoparticle formulation had good biocompatibility and low cytotoxicity before loading PTX. The therapeutic efficacy of CTX-PTX-NP in U-118 MG cells was greater than that of free PTX. Furthermore, cellular uptake of NPs was improved after conjugation with CTX. The CP6C copolymer coated IONPs can be potentially used as a platform for loading and delivery of many hydrophobic drugs and can be easily modified with other ligands for targeting and imaging purposes.

■ ASSOCIATED CONTENT

Ⓢ Supporting Information

Detailed experimental procedures. This material is available free of charge via the Internet at http://pubs.acs.org.

■ AUTHOR INFORMATION

Corresponding Author

*E-mail: mzhang@uw.edu. Fax: (206) 543-3100.

Author Contributions

§These authors contributed equally (M.-H.H. and Q.M.).

Notes

The authors declare no competing financial interest.

■ ACKNOWLEDGMENTS

The work is supported by NIH grants R01CA161953 and R01CA134213. Q.M. and Z.S. acknowledge the support from an NIH Ruth L. Kirschstein T32 Fellowship (T32CA138312). M.H. acknowledges Ministry of Science and Technology (MOST) in Taiwan for funding support for visiting exchange

DOI: 10.1021/acsmacrolett.5b00091
ACS Macro Lett. 2015, 4, 403−407

at University of Washington (Grant ID No. NSC 103-2917-I-009-176).

■ ABBREVIATIONS

CLSM, confocal laser scanning microscopy; CP6C, hexanoyl-chitosan-PEG; CP, methoxy PEG-chitosan; CTX, chlorotoxin; CTX-PTX-NP, chlorotoxin conjugated and paclitaxel loaded iron oxide nanoparticles; DMSO, dimethyl sulfoxide; EE%, encapsulation efficiency; FT-IR, Fourier transform infrared spectroscopy; GBM, glioblastoma; HPLC, high-performance liquid chromatography; IONPs, iron oxide nanoparticles; MMP-2, matrix metalloproteinase-2; mPEG, methoxy PEG; MRI, magnetic resonance imaging; NMR, nuclear magnetic resonance; NPs, nanoparticles; OA-IONP, oleic acid-stabilized iron oxide NPs; PBS, phosphate buffer saline; PEG, polyethylene glycol; PTX, paclitaxel; TEM, transmission electron microscopy

■ REFERENCES

(1) Weiner, N.; Martin, F.; Riaz, M. *Drug Dev. Ind. Pharm.* **1989**, *15*, 1523.
(2) Torchilin, V. P. *Expert Opin. Ther. Pat.* **2005**, *15*, 63.
(3) Sharma, A.; Sharma, U. S. *Int. J. Pharm.* **1997**, *154*, 123.
(4) Kim, S.; Shi, Y. Z.; Kim, J. Y.; Park, K.; Cheng, J. X. *Expert Opin. Drug Delivery* **2010**, *7*, 49.
(5) Gregoriadis, G. *Trends Biotechnol.* **1995**, *13*, 527.
(6) Alexis, F.; Rhee, J.-W.; Richie, J. P.; Radovic-Moreno, A. F.; Langer, R.; Farokhzad, O. C. *Urol. Oncol.: Semin. Orig. Invest.* **2008**, *26*, 74.
(7) Veiseh, O.; Kievit, F. M.; Ellenbogen, R. G.; Zhang, M. Q. *Adv. Drug Delivery Rev.* **2011**, *63*, 582.
(8) Kievit, F. M.; Zhang, M. Q. *Acc. Chem. Res.* **2011**, *44*, 853.
(9) Xie, J.; Xu, C.; Kohler, N.; Hou, Y.; Sun, S. *Adv. Mater.* **2007**, *19*, 3163.
(10) Shen, T.; Weissleder, R.; Papisov, M.; Bogdanov, A.; Brady, T. J. *Magn. Reson. Med.* **1993**, *29*, 599.
(11) Shtykova, E. V.; Huang, X.; Remmes, N.; Baxter, D.; Stein, B.; Dragnea, B.; Svergun, D. I.; Bronstein, L. M. *J. Phys. Chem. C* **2007**, *111*, 18078.
(12) Kievit, F. M.; Veiseh, O.; Bhattarai, N.; Fang, C.; Gunn, J. W.; Lee, D.; Ellenbogen, R. G.; Olson, J. M.; Zhang, M. Q. *Adv. Funct. Mater.* **2009**, *19*, 2244.
(13) Kievit, F. M.; Stephen, Z. R.; Veiseh, O.; Arami, H.; Wang, T. Z.; Lai, V. P.; Park, J. O.; Ellenbogen, R. G.; Disis, M. L.; Zhang, M. Q. *ACS Nano* **2012**, *6*, 2591.
(14) Dash, M.; Chiellini, F.; Ottenbrite, R. M.; Chiellini, E. *Prog. Polym. Sci.* **2011**, *36*, 981.
(15) Khor, E.; Lim, L. Y. *Biomaterials* **2003**, *24*, 2339.
(16) Dodane, V.; Vilivalam, V. D. *Pharm. Sci. Technol.* **1998**, *1*, 246.
(17) Prabaharan, M.; Mano, J. F. *Drug Delivery* **2005**, *12*, 41.
(18) Mao, S.; Sun, W.; Kissel, T. *Adv. Drug Delivery Rev.* **2010**, *62*, 12.
(19) Bhattarai, N.; Gunn, J.; Zhang, M. *Adv. Drug Delivery Rev.* **2010**, *62*, 83.
(20) Veiseh, O.; Sun, C.; Fang, C.; Bhattarai, N.; Gunn, J.; Kievit, F.; Du, K.; Pullar, B.; Lee, D.; Ellenbogen, R. G.; Olson, J.; Zhang, M. *Cancer Res.* **2009**, *69*, 6200.
(21) Deshane, J.; Garner, C. C.; Sontheimer, H. *J. Biol. Chem.* **2003**, *278*, 4135.
(22) Harris, J. M.; Struck, E. C.; Case, M. G.; Paley, M. S.; Yalpani, M.; Van Alstine, J. M.; Brooks, D. E. *J. Polym. Sci., Polym. Chem. Ed.* **1984**, *22*, 341.
(23) Bhattarai, N.; Matsen, F. A.; Zhang, M. *Macromol. Biosci.* **2005**, *5*, 107.
(24) Kumirska, J.; Czerwicka, M.; Kaczyński, Z.; Bychowska, A.; Brzozowski, K.; Thöming, J.; Stepnowski, P. *Mar. Drugs* **2010**, *8*, 1567.
(25) Weinhold, M. X.; Sauvageau, J. C. M.; Keddig, N.; Matzke, M.; Tartsch, B.; Grunwald, I.; Kubel, C.; Jastorff, B.; Thoming, J. *Green Chem.* **2009**, *11*, 498.
(26) Bo, L.; Xiaoyun, L.; Canfeng, Z.; Xiaoying, W.; Runcang, S. *Nanotechnology* **2013**, *24*, 235601.
(27) Verma, A.; Stellacci, F. *Small* **2010**, *6*, 12.
(28) Chen, H.; Kim, S.; Li, L.; Wang, S.; Park, K.; Cheng, J.-X. *Proc. Natl. Acad. Sci. U.S.A.* **2008**, *105*, 6596.
(29) Gabizon, A.; Dagan, A.; Goren, D.; Barenholz, Y.; Fuks, Z. *Cancer Res.* **1982**, *42*, 4734.
(30) Clary, L.; Verderone, G.; Santaella, C.; Vierling, P. *Biochim. Biophys. Acta, Biomembr.* **1997**, *1328*, 55.
(31) Immordino, M. L.; Brusa, P.; Arpicco, S.; Stella, B.; Dosio, F.; Cattel, L. *J. Controlled Release* **2003**, *91*, 417.

DOI: 10.1021/acsmacrolett.5b00091
ACS Macro Lett. 2015, 4, 403−407